Presented at the 23rd Annual CMAS Conference, Chapel Hill, NC, October 21, 2024

Enhancing Meteorological and Air Quality Prediction Accuracy through High-Resolution Data Assimilation Using Deep Learning

Hossein Alizadeh , Ali Azimi , Seyed Hamid Delbari , Vahid Hosseini*

School of Sustainable Energy Engineering, Simon Fraser university, V3T 0N1, British Columbia, Canada

1. INTRODUCTION

High resolution meteorological and air quality forecasts are needed for environmental management and public health. Traditional models like the Weather Research and Forecasting (WRF) model often struggle to capture small-scale meteorological phenomena in complex terrains and urban areas like Edmonton, Canada, known for its extreme cold climate. These limitations arise from inadequate meso-scale resolutions that cannot resolve finer-scale processes such as eddies and turbulence occurring over meters to kilometers (Holtslag et al., 2013; Wiersema et al., 2020) and challenges in representing complex interactions between energy balance, topography, and boundary-layer dynamics (Jfworrek et al., 2023). The limitations lead to inaccurate predictions of near-surface air quality, especially regarding pollutant distributions.

While increasing model resolution using large-eddy simulation (LES) techniques resolves small-scale processes within the planetary boundary layer (PBL), this approach is computationally intensive and limited by incomplete understanding of stable PBL physics (Bao et al., 2018; Crosman & Horel, 2017; Liu et al., 2020).

An alternative, more computationally efficient method is four-dimensional data assimilation (FDDA), or "nudging," which adjusts models toward observations or gridded-analysis data through dynamical relaxation without violating meteorological consistency (Deng et al., 2009; Reen, 2016; Stauffer et al., 1991). FDDA methods in WRF, including analysis (grid) nudging and observational nudging, have shown improvements in meteorological simulations and subsequent air quality predictions (Desamsetti et al., 2022; Spero et al., 2018; Wang & Cui, 2018). However, analysis nudging may negatively impact simulations of humidity and wind speed (Ma et al., 2016; Tran et al., 2018). Observational nudging has effectively improved simulations of surface temperature, wind fields, and PBL height, leading to better air quality forecasts (J. Li et al., 2022; X. Li et al., 2016).

Data-driven techniques like deep learning have emerged to enhance the data assimilation process in meteorology and air quality fields by capturing nonlinear relationships and patterns that traditional methods lack (Huang et al., 2023; Niu et al., 2024). This capability offers potential improvements in representing micro-scale atmospheric processes, particularly in complex terrains and under stable atmospheric conditions (Guo et al., 2024; He et al., 2023).

This study introduces a Residual Encoder-Decoder model with an attention mechanism to generate high-resolution (1.33 km) gridded data by downscaling coarser datasets. The model is trained in two stages: first, it downscales from the NCEP Final Analysis at 1-degree (~108 km) resolution to the NCEP North America Mesoscale (NAM) at 12 km resolution over the Edmonton domain to learn essential patterns. It uses the learned weights to downscale from the 12 km grid to a 1.33 km grid without direct fine-scale data. By employing residual learning, the model predicts differences between interpolated low-resolution data and the high-resolution target, refining details and avoiding overfitting. The attention mechanism enhances prediction accuracy by focusing on relevant spatial features in the refined domain.

The high-resolution data generated by the deep learning model are assimilated into the WRF model using observational nudging. This assimilation aims to improve meteorological predictions by reducing biases in temperature, wind speed, wind direction, and relative humidity—parameters crucial during extreme weather events characteristic of Edmonton's climate. Additionally, the Community Multiscale Air Quality (CMAQ) model is utilized to assess how the improved meteorological fields enhance the prediction of air pollutant concentrations, specifically $PM_{2.5}$ and ozone, within the study area. By integrating advanced data-driven techniques with traditional meteorological models, this study bridges the gap between the availability of coarse-resolution data

**Corresponding author:* Vahid Hosseini, School of Sustainable Energy Engineering, Simon Fraser university, V3T 0N1, British Columbia, Canada; e-mail: vahid_hosseini@sfu.ca

and the need for high-resolution predictions. The proposed approach enhances both meteorological and air quality prediction accuracy, offering a valuable tool for environmental forecasting in regions with complex weather patterns.

2. PROBLEM DEFINITION, MODEL & METHODOLOGY

2.2 Model Domain

The study area is the City of Edmonton in Alberta province in Canada. To better capture the topographical features of the study area and their impacts on the local atmospheric process, three two-way nested domains with increasing grid resolution is used in WRFv4.5. The largest domain at 9 km grid resolution, covers the majority of the Alberta, Southeast of British Columbia and Eastern Saskatchewan. The two inner domains cover the Greater Edmonton Area (GEA) and the City of Edmonton at 3km and 1km spatial resolution, respectively (Fig. **1**).

This approach is recommended to reduce the effect of the coarse boundary values, fed into the largest domain, on the intermediate and innermost domains, improving the prediction accuracy of the model (Malakar et al., 2012).

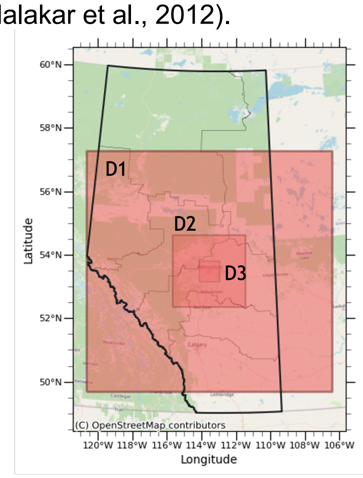

Fig. 1: Nested Computational Domain over Alberta, Canada

2.2 WRF-CMAQ Setup

The Weather Research and Forecasting (WRF) model v4.5 (Skamarock et al., 2019) is used to simulate meteorological parameters such as temperature, relative humidity, wind speed, and wind direction over the study area. WRF offers a variety of physics schemes to capture the complex interactions of atmospheric processes. For this study, the Thompson scheme (Thompson et al., 2004) is used for microphysics parameterization, while long- and short-wave radiation were resolved using the Rapid Radiative Transfer Model for Global Climate Models (RRTMG) schemes (Iacono et al., 2008). Additionally, the revised MM5 scheme (Jiménez et al., 2012) and the Unified Noah Land Surface Model (Tewari and Coauthors 2004) are selected to represent the surface layer and land surface fluxes within the domain. Finally, the Yonsei University scheme is applied to model horizontal and vertical mixing near the surface and within the planetary boundary layer (Hong et al., 2006). The Global Forecast System (GFS) weather analysis data of the National Center for Environmental Protection (NCEP) is used for initialization and boundary values of the coarsest domain. WRF in-house data assimilation module is deployed to nudge the prognostic variables toward the observation data which will be explained in detail in the following section.

The air quality scenarios are conducted using the Community Multiscale Air Quality (CMAQ V5.4) modeling framework. CMAQ integrates meteorological data, emissions inventories, and detailed chemical mechanisms to model the transport, transformation, and deposition of atmospheric pollutants such as ozone, particulate matter, and air toxics. The model employs Piecewise Parabolic Method (PPM) for advection processes (Colella & Woodward, 1984), Eddy Diffusion theory (SMAGORINSKY, 1963) to account for the horizontal diffusion fluxes and the Euler Backward Iterative (EBI)(Hertel et al., 1993) method for solving stiff chemical kinetics. The gas-phase and aerosol-phase chemistry in this study are represented with the Carbon Bond 6 (CB6) and the Aerosol Module 7 (AE7), respectively. The boundary and initial condition for the CMAQ domain are generated using the northern hemisphere monthly modeling results of CMAQ available online through the CMAS Center database. The anthropogenic emission data are acquired from the latest Alberta's emission inventory compiled by the NOVUS Env. and RAMBOLL for the base year 2013 (Nopmongcol et al., 2018) and prepared by EPA's SMOKE V5.0 for the CMAQ. The biogenic emissions are processed inline using the Biogenic Emission Inventory System (BEIS V4.0). Finally, the WRF-CMAQ was setup in a one-way (decoupled) approach.

2.4. Data-driven Weather Downscaling Model

A Residual Encoder-Decoder model with an Attention Mechanism is utilized to downscale weather variables, including temperature, wind speed, wind direction, and relative humidity at the surface level. The model downscales data from the coarser NAM (12 km) analysis resolution to high-resolution (1.33 km) input, which is used to nudge the WRF forecast for the finest domain ove r Edmonton. This approach is inspired by the work of Serifi et al.(Serifi et al., 2021), who employed a UNET-based neural network for spatiotemporal downscaling of climate data.

The training process consists of two stages. First, the model is trained on 108 km GFS data to reconstruct the 12 km NAM analysis, allowing it to capture the general features of the dataset. Afterward, the model downscales the NAM analysis to 1.33 km resolution using the learned weights. The Encoder-Decoder architecture captures critical low-resolution features via the encoder and reconstructs high-resolution outputs through the decoder. Incorporating the Attention Mechanism directs the model's focus to the most relevant spatial details during the downscaling, improving accuracy by emphasizing fine-grained feature.

To enhance efficiency and accuracy, the model employs Residual Learning. Instead of predicting the high-resolution data outright, the model first generates an initial estimate using bilinear interpolation. The residual component, representing the difference between the bilinear interpolation and the true high-resolution data, is predicted by the model. This approach simplifies the learning task by focusing on fine-tuning the bilinear interpolation, mitigating overfitting risks. The final high-resolution output is given by:

$$\widehat{f^{-1}}(X) = \widehat{f^{-1}}(X)_{\text{bilinear interpolation}} + r\left(\widehat{f^{-1}}(X)\right)_{\text{residual}} \quad \text{Eq. 1}$$

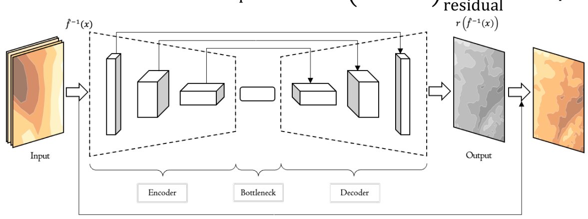

Fig. 2: The Architecture of the Residual Encoder-Decoder Climate Downscaling Model

Model performance was validated using the Root Mean Squared Error (RMSE) and the Coefficient of Determination (R^2), measuring prediction accuracy and the proportion of explained variance, respectively.

2.5 Modeling Scenario

To improve the predicted concentrations of criteria air contaminants (CACs) by CMAQ over Edmonton during the summer period from July 10 to July 22, 2019, we fine-tuned WRF predictions using the nudging technique implemented in the WRF Data Assimilation module (Reen, 2016). WRF provides two primary methods for nudging: observation nudging (ON) and analysis nudging (AN). These techniques relax the meteorological variables in each grid point at regular intervals, based on the availability of nudging data.

Three scenarios were designed to evaluate the impact of nudging the innermost domain on both WRF and CMAQ predictions. The first scenario serves as a reference with no nudging applied to the meteorological data (NON). In the second scenario, the AN method is applied to nudge WRF output at the surface level toward NCEP NAM 12 km analysis data (AN-NAM). In the third scenario, higher-resolution analysis data with a 1.33 km grid spacing—generated by the weather downscaling model described in Section 2.4—were used as input for observation nudging (ON-DD). The third scenario aims to assess the advantages of using the high-res downscaled model data compared to the coarse grid analysis used in the second scenario for nudging applications. The nudging coefficients for AN-NAM and ON-DD cases are set according to the WRF-DA guidelines.

3. RESULTS & DISCUSSION

3.1 Data-driven Downscaling Output

The NCEP GFS (108 km) and NAM (12 km) analyses at 6-hr intervals for the entire 2019 is used to train the downscaling model over the Edmonton domain. In particular, the model is trained to downscale the temperature, horizontal wind speed components and the relative humidity parameters which are subsequently used for data ingestion in the ON-DD scenario. Table **1** shows the performance metric of the model for the corresponding parameters over the validation dataset.

Table 1: Downscaling Performance Metrics for the Surface Weather Parameters

Parameter	**MAB**	**RMSE**	**R^2**
Temp. (˚C)	0.94	1.24	98.4
Wind (U Comp.) (ms^{-1})	0.34	0.58	93.1
Wind (V Comp.) (ms^{-1})	0.44	0.65	91.8

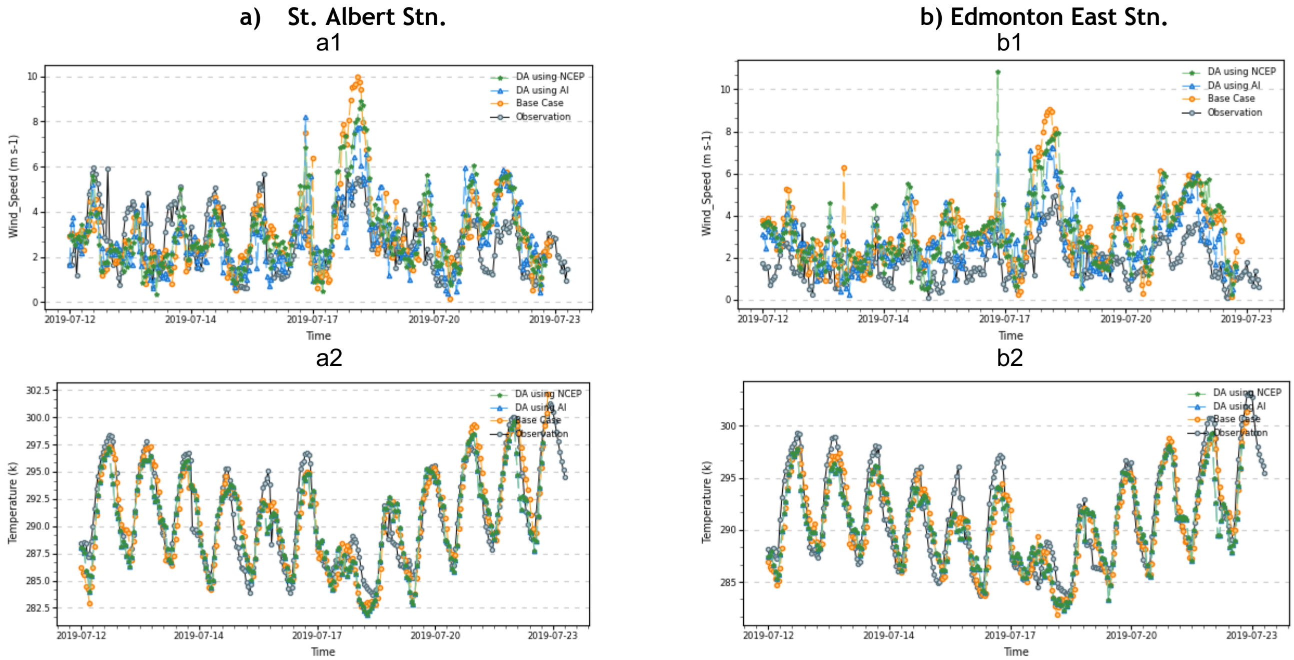

Fig. 3: The Timeseries of Surface Wind Speed and Temperature for: a) St. Albert Stn., b) Edmonton East Stn.

3.2 Impacts of the Nudging on the WRF Output

To evaluate the performance of the three scenarios, ground-level WRF outputs were compared with surface observations from 12 weather and air quality monitoring stations across Edmonton. Hourly surface-level temperature, wind speed, wind direction, and relative humidity were compared with the corresponding WRF output values. **Fig. 3** presents the time series of temperature and wind speed at the St. Albert and Edmonton East stations, located in the northwest and East of Edmonton, respectively. The AN-NAM and ON-DD cases resulted in lower mean bias error (MBE) and root mean square error (RMSE) values for surface wind speed; however, the latter exhibited a slightly poorer performance in the correlation score compared to the AN-NAM case and the reference case without nudging (NON). At the St. Albert station, the wind speed MBE was reduced from 1.21 m/s to 1.13 m/s and 1.05 m/s for the AN-NAM and ON-DD cases, respectively. Similarly, the mean bias error for wind speed at the Edmonton East station decreased from 1.47 m/s to 1.41 m/s and 1.27 m/s for the corresponding scenarios. **Fig. 3a1** and **Fig. 3b1** illustrate the effects of nudging in mitigating the episodic overestimation and underestimation of hourly wind speed values observed at ground level. Overall, the ON-DD case performed slightly better than both the AN-NAM and NON cases in predicting surface wind speed, highlighting the positive impact of

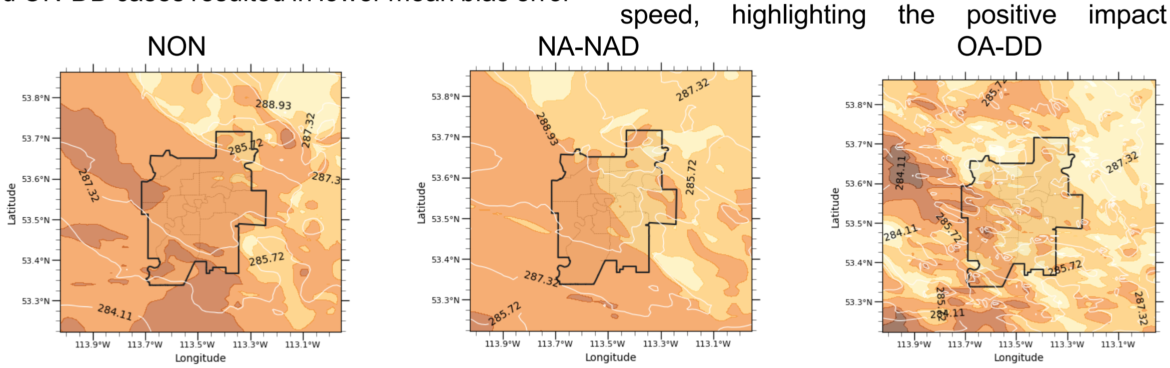

Fig. 4: Comparison of the Temperature (White Lines) and Wind Speed Contours Over the Edmonton resolved by a) NON, b) NA-NAM, c) OA-DD cases

incorporating high-resolution downscaling output into the nudging analysis.

Similar to wind speed, the NA-NAM and OA-DD cases improved the MBE and RMSE for surface temperature at the St. Albert station (**Fig. 3a2**) without negatively impacting the correlation score. The mean bias at St. Albert improved from 1.51°C to 1.43°C and 1.37°C for the NA-NAM and OA-DD cases, respectively. However, the NA-NAM case performed worse than both the NON and OA-DD cases in predicting temperature at the Edmonton East station, with an MBE of 1.81°C compared to 1.78°C for NON and 1.73°C for OA-DD (**Fig. 3b2**).

Error! Reference source not found. illustrates the contours of temperature (white lines) and wind speed (colored shading) for the innermost WRF domain over Edmonton on July 18, 2019. It is evident that ingesting the high-resolution downscaling data (OA-DD) enables the WRF to better capture complex, fine-scale momentum fluxes and surface temperature compared to the NON and NA-NAM cases.

3.3 Impacts of the Nudging on the CMAQ outputs.

The hourly concentrations of $PM_{2.5}$, O_3, NO_2, and at the St. Albert and Edmonton East stations were compared with the corresponding hourly-averaged surface concentration outputs from CMAQ for the reference (NON) and OA-DD cases discussed earlier.

Table 2: Comparison of CMAQ performance improvement under the NON and OA-DD scenarios for $PM_{2.5}$, NO_2, and O_3

		St. Albert			Edmonton East		
		MAPE	**RMSE**	**IOA**	**MAPE**	**RMSE**	**IOA**
NON	$PM_{2.5}$ *	0.47	7.7	0.40	0.45	7.7	0.33
	O_3 **	0.15	0.008	0.82	0.18	0.009	0.71
	NO_2 **	0.81	0.01	0.52	0.68	0.009	0.45
OA-DD	$PM_{2.5}$ *	0.42	5.8	0.62	0.43	6.2	0.55
	O_3 **	0.14	0.007	0.83	0.16	0.008	0.75
	NO_2 **	0.75	0.008	0.58	0.71	0.009	0.49

* The unit is ($\mu g/m^3$)
** The unit is ppm

A comparison between the impact of meteorology field from NON and OA-DD scenarios on the CMAQ output for $PM_{2.5}$, NO_2, and O_3 concentrations (Table **2**) reveals improvements in model performance for the latter across all the metrics. For $PM_{2.5}$, the OA-DD case shows a decrease in mean absolute percentage error (MAPE) (0.47 to 0.42 at St. Albert, 0.45 to 0.43 at Edmonton East), RMSE (7.7 to 5.8, and 7.7 to 6.2, respectively), and a substantial increase in index of agreement (IOA) (0.40 to 0.62, 0.33 to 0.55), indicating better alignment with observed values. Similar improvements are seen for NO_2, where MAPE drops (0.81 to 0.75 at St. Albert, 0.68 to 0.71 at Edmonton East), RMSE remains largely unchanged, but IOA improves (0.52 to 0.58, and 0.45 to 0.49). For O_3, the OA-DD scenario reduces MAPE slightly (0.15 to 0.14 at St. Albert, 0.18 to 0.16 at Edmonton East), decreases RMSE marginally, and increases IOA (0.82 to 0.83, and 0.71 to 0.75), showing overall improved model performance across all pollutants and metrics with the improved surface meteorology outputted by OA-DD scenario.

4. SUMMARY AND CONCLUSION

This study enhanced meteorological and air quality predictions over Edmonton by integrating high-resolution data assimilation using a deep learning approach. A Residual Encoder-Decoder model with an attention mechanism was developed to downscale coarse-resolution weather data to a 1.33 km resolution. The model was trained in two stages: first, downscaling from the NCEP Final Analysis at approximately 108 km to the NAM at 12 km to capture essential patterns; second, using the learned weights to downscale from 12 km to 1.33 km without direct fine-scale data.

The high-resolution data generated were assimilated into the WRF model using observational nudging (ON-DD scenario) and compared with scenarios of no nudging (NON) and analysis nudging using NAM data (AN-NAM). The ON-DD scenario demonstrated significant improvements in predicting surface meteorological variables and air pollutant concentrations.

At the St. Albert station, the mean bias error (MBE) for wind speed decreased from 1.21 m/s (NON) to 1.05 m/s (ON-DD), and for temperature, the MBE improved from 1.51°C to 1.37°C. At the Edmonton East station, wind speed MBE reduced from 1.47 m/s to 1.27 m/s, and temperature MBE improved from 1.78°C to 1.73°C.

For air quality predictions, the ON-DD scenario reduced the mean absolute percentage error (MAPE) for $PM_{2.5}$ concentrations from 0.47 (NON) to 0.42 at St. Albert and from 0.45 to 0.43 at Edmonton East. The root mean square error (RMSE) for $PM_{2.5}$ decreased from 7.7 $\mu g/m^3$ to 5.8 $\mu g/m^3$ at St. Albert and from 7.7 $\mu g/m^3$ to 6.2 $\mu g/m^3$ at Edmonton East. The index of agreement (IOA) for $PM_{2.5}$ increased from 0.40 to 0.62 and from 0.33 to 0.55, respectively.

In conclusion, integrating high-resolution, deep learning downscaled data into meteorological models significantly enhances the accuracy of weather and air quality predictions, effectively bridging the gap between coarse-resolution data and the need for high-resolution forecasts in complex regions.

5. REFERENCES

Alexandru, A., de Elia, R., Laprise, R., Separovic, L., & Biner, S. (2009). Sensitivity Study of Regional Climate Model Simulations to Large-Scale Nudging Parameters. *Monthly Weather Review*, *137*(5), 1666–1686. https://doi.org/10.1175/2008MWR2620.1.10.1175/2008MWR2620.1

Bao, J., Chow, F. K., & Lundquist, K. A. (2018). Large-Eddy Simulation over Complex Terrain Using an Improved Immersed Boundary Method in the Weather Research and Forecasting Model. *Monthly Weather Review*, *146*(9), 2781–2797. https://doi.org/10.1175/MWR-D-18-0067.1

Bowden, J. H., Otte, T. L., Nolte, C. G., & Otte, M. J. (2012). Examining Interior Grid Nudging Techniques Using Two-Way Nesting in the WRF Model for Regional Climate Modeling. *Journal of Climate*, *25*(8), 2805–2823. https://doi.org/10.1175/JCLI-D-11-00167.1.10.1175/JCLI-D-11-00167.1

Chen, Y., Fung, J. C. H., Yuan, D., Chen, W., Fung, T., & Lu, X. (2023). Development of an integrated machine-learning and data assimilation framework for NOx emission inversion. *Science of The Total Environment*, *871*, 161951. https://doi.org/10.1016/J.SCITOTENV.2023.161951

Colella, P., & Woodward, P. R. (1984). The Piecewise Parabolic Method (PPM) for gas-dynamical simulations. *Journal of Computational Physics*, *54*(1), 174–201. https://doi.org/10.1016/0021-9991(84)90143-8

Crosman, E. T., & Horel, J. D. (2017). Large-eddy simulations of a Salt Lake Valley cold-air pool. *Atmospheric Research*, *193*, 10–25. https://doi.org/10.1016/J.ATMOSRES.2017.04.010

Deng, A., Stauffer, D., Gaudet, B., Dudhia, J., Hacker, J., Bruyere, C., Wu, W., Vandenberghe, F., Liu, Y., & Bourgeois, A. (2009). 1.9 Update on WRF-ARW End-to-End Multi-Scale FDDA System. *WRF Users' Workshop: Boulder, CO, USA*.

Desamsetti, S., Dasari, H. P., Langodan, S., Viswanadhapalli, Y., Attada, R., Luong, T. M., Knio, O., Titi, E. S., & Hoteit, I. (2022). Enhanced Simulation of the Indian Summer Monsoon Rainfall Using Regional Climate Modeling and Continuous Data Assimilation. *Frontiers in Climate*, *4*. https://doi.org/10.3389/FCLIM.2022.817076

Guo, S., Yang, Y., & Liu, P. (2024). Assimilation of the deep learning-corrected global forecast system fields into the regional model for improving medium-range persistent precipitation forecasts. *Atmospheric Research*, *303*, 107318. https://doi.org/10.1016/J.ATMOSRES.2024.107318

He, X., Li, Y., Liu, S., Xu, T., Chen, F., Li, Z., Zhang, Z., Liu, R., Song, L., Xu, Z., Peng, Z., & Zheng, C. (2023). Improving regional climate simulations based on a hybrid data assimilation and machine learning method. *Hydrology and Earth System Sciences*, *27*(7), 1583–1606. https://doi.org/10.5194/HESS-27-1583-2023

Hertel, O., Berkowicz, R., Christensen, J., & Hov, Ø. (1993). Test of two numerical schemes for use in atmospheric transport-chemistry models. *Atmospheric Environment. Part A. General Topics*, *27*(16), 2591–2611. https://doi.org/10.1016/0960-1686(93)90032-T

Holtslag, A. A. M., Svensson, G., Baas, P., Basu, S., Beare, B., Beljaars, A. C. M., Bosveld, F. C., Cuxart, J., Lindvall, J., Steeneveld, G. J., Tjernström, M., & Van De Wiel, B. J. H. (2013). Stable Atmospheric Boundary Layers and Diurnal Cycles: Challenges for Weather and Climate Models. *Bulletin of the American Meteorological Society*, *94*(11), 1691–1706. https://doi.org/10.1175/BAMS-D-11-00187.1

Hong, S. Y., Noh, Y., & Dudhia, J. (2006). A New Vertical Diffusion Package with an Explicit Treatment of Entrainment Processes. *Monthly Weather Review*, *134*(9), 2318–2341. https://doi.org/10.1175/MWR3199.1

Huang, C., Niu, T., Wu, H., Qu, Y., Wang, T., Li, M., Li, R., & Liu, H. (2023). A Data Assimilation Method Combined with Machine Learning and Its Application to Anthropogenic Emission Adjustment in CMAQ. *Remote Sensing 2023, Vol. 15, Page 1711*, *15*(6), 1711. https://doi.org/10.3390/RS15061711

Iacono, M. J., Delamere, J. S., Mlawer, E. J., Shephard, M. W., Clough, S. A., & Collins, W. D. (2008). Radiative forcing by long-lived greenhouse gases: Calculations with the AER radiative transfer models. *Journal of Geophysical Research: Atmospheres*, *113*(D13), 13103. https://doi.org/10.1029/2008JD009944

Jiménez, P. A., Dudhia, J., González-Rouco, J. F., Navarro, J., Montávez, J. P., & García-Bustamante, E. (2012). A Revised Scheme for the WRF Surface Layer Formulation. *Monthly Weather Review*, *140*(3), 898–918. https://doi.org/10.1175/MWR-D-11-00056.1

Li, J., Yu, S., Chen, X., Zhang, Y., Li, M., Li, Z., Song, Z., Liu, W., Li, P., Xie, M., & Xing, J. (2022). Evaluation of the WRF-CMAQ Model Performances on Air Quality in China with the Impacts of the Observation Nudging on Meteorology. *Aerosol and Air Quality Research*, *22*(4), 220023. https://doi.org/10.4209/AAQR.220023

Li, X., Choi, Y., Czader, B., Roy, A., Kim, H., Lefer, B., & Pan, S. (2016). The impact of observation nudging on simulated meteorology and ozone concentrations during DISCOVER-AQ 2013 Texas campaign. *Atmospheric Chemistry and Physics*, *16*(5), 3127–3144. https://doi.org/10.5194/ACP-16-3127-2016

Li, X., & Rappenglück, B. (2014). A WRF–CMAQ study on spring time vertical ozone structure in Southeast Texas. *Atmospheric Environment*, *97*, 363–385. https://doi.org/10.1016/J.ATMOSENV.2014.08.036

Liu, Y., Liu, Y., Muñoz-Esparza, D., Hu, F., Yan, C., & Miao, S. (2020). Simulation of Flow Fields in Complex Terrain with WRF-LES: Sensitivity Assessment of Different PBL Treatments. *Journal of Applied Meteorology and Climatology*, *59*(9), 1481–1501. https://doi.org/10.1175/JAMC-D-19-0304.1

Ma, Y., Yang, Y., Mai, X., Qiu, C., Long, X., & Wang, C. (2016). Comparison of Analysis and Spectral Nudging Techniques for Dynamical Downscaling with the WRF Model over China. *Advances in Meteorology*, *2016*(1), 4761513. https://doi.org/10.1155/2016/4761513

Malakar, P., Saxena, V., George, T., Mittal, R., Kumar, S., Naim, A. G., & Husain, S. A. B. H. (2012). Performance Evaluation and Optimization of Nested High Resolution Weather Simulations. *Lecture Notes in Computer Science (Including Subseries Lecture Notes in Artificial Intelligence and Lecture Notes in Bioinformatics)*, *7484 LNCS*, 805–817. https://doi.org/10.1007/978-3-642-32820-6_80

Niu, Z., Huang, W., Zhang, L., Deng, L., Wang, H., Yang, Y., Wang, D., & Li, H. (2024). *Improving Typhoon Predictions by Integrating Data-Driven Machine Learning Models with Physics Models Based on the Spectral Nudging and Data Assimilation*. https://arxiv.org/abs/2408.12630v1

Reen, B. (2016). A brief guide to observation nudging in WRF. *Battlefield Environment Division, Army Research Laboratory*.

Serifi, A., Günther, T., & Ban, N. (2021). Spatio-Temporal Downscaling of Climate Data Using Convolutional and Error-Predicting Neural Networks. *Frontiers in Climate*, *3*, 656479. https://doi.org/10.3389/FCLIM.2021.656479/BIBTEX

Skamarock, C., Klemp, B., Dudhia, J., Gill, O., Liu, Z., Berner, J., Wang, W., Powers, G., Duda, G., Barker, D. M., & Huang, X. (2019). *A Description of the Advanced Research WRF Model Version 4*. https://api.semanticscholar.org/CorpusID:196211930

SMAGORINSKY, J. (1963). GENERAL CIRCULATION EXPERIMENTS WITH THE PRIMITIVE EQUATIONS: I. THE BASIC EXPERIMENT. *Monthly Weather Review*, *91*(3), 99–164. https://doi.org/10.1175/1520-0493(1963)091<0099:GCEWTP>2.3.CO;2

Spero, T. L., Nolte, C. G., Mallard, M. S., & Bowden, J. H. (2018). A Maieutic Exploration of Nudging Strategies for Regional Climate Applications Using the WRF Model. *Journal of Applied Meteorology and Climatology*, *57*(8), 1883–1906. https://doi.org/10.1175/JAMC-D-17-0360.1

Stauffer, D. R., Seaman, N. L., & Binkowski, F. S. (1991). Use of four-dimensional data assimilation in a limited-area mesoscale model Part II: effects of data assimilation within the planetary boundary layer. *Monthly Weather Review*, *119*(3), 734–754. https://doi.org/10.1175/1520-0493(1991)119<0734:UOFDDA>2.0.CO;2

Tewari, M., & Coauthors. (2004). Implementation and verification of the unified Noah land-surface model in the WRF model. *20th Conference on Weather Analysis and Forecasting/16th*

Conference on Numerical Weather Prediction. https://opensky.ucar.edu/islandora/object/conference%3A1576

Thompson, G., Rasmussen, R. M., & Manning, K. (2004). Explicit Forecasts of Winter Precipitation Using an Improved Bulk Microphysics Scheme. Part I: Description and Sensitivity Analysis. *Monthly Weather Review*, *132*(2), 519–542. https://doi.org/10.1175/1520-0493(2004)132<0519:EFOWPU>2.0.CO;2

Tran, T., Tran, H., Mansfield, M., Lyman, S., & Crosman, E. (2018). Four dimensional data assimilation (FDDA) impacts on WRF performance in simulating inversion layer structure and distributions of CMAQ-simulated winter ozone concentrations in Uintah Basin. *Atmospheric Environment*, *177*, 75–92. https://doi.org/10.1016/J.ATMOSENV.2018.01.012

Nopmongcol, U., Johnson, J., Shah, T., Vennam, P., Trail, M., & Morris, R. (2018). *Provincial Air Quality Photochemical Modelling*.

Wang, C., & Cui, Z. (2018). Improvement of short-term climate prediction with indirect soil variables assimilation in China. *Journal of Climate*, *31*(4), 1399–1412. https://doi.org/10.1175/JCLI-D-17-0210.1

Wiersema, D. J., Lundquist, K. A., & Chow, F. K. (2020). Mesoscale to Microscale Simulations over Complex Terrain with the Immersed Boundary Method in the Weather Research and Forecasting Model. *Monthly Weather Review*, *148*(2), 577–595. https://doi.org/10.1175/MWR-D-19-0071.1